Accepted by ApJ October 8, 2006

Neon Fine-Structure Line Emission By X-ray Irradiated Protoplanetary Disks

Alfred E. Glassgold

Astronomy Department, University of California, Berkeley, CA 94720

aglassgold@astron.berkeley.edu

Joan R. Najita

NOAO, 950 N. Cherry Avenue, Tucson, AZ 85719

najita@noao.edu

Javier Igea

Vatican Observatory, V-00120 Cittá del Vaticano

jigea@telefonica.net

ABSTRACT

Using a thermal-chemical model for the generic T-Tauri disk of D'Alessio *et al.* (1999), we estimate the strength of the fine-structure emission lines of Ne II and Ne III at 12.81 and 15.55 μm that arise from the warm atmosphere of the disk exposed to hard stellar X-rays. The Ne ions are produced by the absorption of keV X-rays from the K shell of neutral Ne, followed by the Auger ejection of several additional electrons. The recombination cascade of the Ne ions is slow because of weak charge transfer with atomic hydrogen in the case of Ne^{++} and by essentially no charge transfer for Ne^{+}. For a distance of 140 pc, the 12.81 μm line of Ne II has a flux $\sim 10^{-14}$erg cm^{-2}s^{-1}, which should be observable with the *Spitzer* Infrared Spectrometer and suitable ground based instrumentation. The detection of these fine-structure lines would clearly demonstrate the effects of X-rays on the physical and chemical properties of the disks of young stellar objects and provide a diagnostic of the warm gas in protoplanetary disk atmospheres. They would complement the observed H_2 and CO emission by probing vertical heights above the molecular transition layer and larger radial distances that include the location of terrestrial and giant planets.

Subject headings: accretion, accretion disks — infrared: stars — planetary systems: protoplanetary disks — stars: formation — stars: pre-main sequence — X-rays: stars

1. Introduction

Young stellar objects (YSOs) are observed to be strong emitters of X-rays (e.g., Feigelson & Montmerle 1999). The X-rays have the potential to affect the physical properties of nearby circumstellar material (e.g., Glassgold, Feigelson & Montmerle 2000) and thus the course of star formation (Silk & Norman 1980; Pudritz & Silk 1987). Tsujimoto *et al.* (2005) observed X-ray fluorescence from cold Fe ions in seven sources in the Orion Nebula Cluster, which they have interpreted to be the result of absorption of hard stellar X-rays by cool circumstellar disk material. This confirmation of the interaction of stellar X-rays with the disks of YSOs raises the question of whether there are specific diagnostics for the effect of X-rays on the physical and chemical properties of these disks, which are believed to play a crucial role in the formation of stars and planets. Although the gas is the main reservoir of mass for much of the lifetime of a YSO disk, much less is known about the gas than the easier to measure dust. Thus we address the issue of X-ray effects in the broader context of the search for gaseous diagnostics of disk gas.

This type of question has a long history in studies of the interstellar medium of our own and external galaxies, where definitive demonstrations of the effects of X-rays have been elusive because other external heating and ionizing radiations, such as UV radiation and cosmic rays, can produce similar effects. Some of the diagnostic possibilities discussed in the literature are multiply charged ions (Dalgarno 1976; Langer 1978); specific molecules, especially ions and radicals (Krolik & Kallmann 1983; Neufeld, Maloney & Conger 1994; Lepp & Dalgarno 1996; Sternberg, Yan & Dalgarno 1997; Yan & Dalgarno 1997); near-infrared H_2 ro-vibrational transitions (Lepp & McCray 1983; Draine & Woods 1989; Gredel & Dalgarno 1995; Tiné *et al.* 1997); and fine-structure lines (Maloney, Hollenbach & Tielens 1996).

Many of these possibilities are now being re-investigated in the context of chemical modeling of the disks and envelopes of YSOs irradiated by X-rays and UV radiation (e.g., Aikawa & Herbst 1999; Markwick *et al.* 2002; Gorti & Hollenbach 2004; Millar & Nomura 2005; Stäuber *et al.* 2005). An important aspect of the X-ray irradiation of protoplanetary disks is that the upper atmosphere close to the YSO is heated to relatively high temperatures $\sim 5,000\,\mathrm{K}$ (Glassgold, Najita & Igea 2004, henceforth GNI04; Alexander, Clarke & Pringle 2004). The temperature then decreases going down towards the disk midplane. The

accompanying thermal-chemical structure consists of a hot partially-ionized atomic layer on top of a cool molecular layer with a much smaller ionization fraction. In between, there is a warm partially-molecular layer with gas temperatures $\sim 500 - 2,000\,\mathrm{K}$. This layered structure of X-ray irradiated disks can be traced back to earlier studies of various astrophysical environments, e.g., Halpern & Grindlay (1983), Krolik & Kallman (1983) and Lepp & McCray (1983). The thermal properties of the disk atmosphere above the cool molecular layer play a critical role in determining the observational signatures of disks.

The potential for ambiguity in the identification of X-ray diagnostics also arises in protoplanetary disks because of the presence of stellar UV radiation which can heat the gas in the surface layers via the photoelectric effect on small grains and polycyclic aromatic hydrocarbons compounds or PAHs (Kamp & Dullemond 2004; Nomura & Millar 2005). In the far outer regions of disks, interstellar UV radiation and galactic cosmic rays may also play a role in heating and ionizing the gas. We suggest that the mid-infrared fine-structure lines of Ne II at 12.81 μm and of Ne III at 15.6 μm may provide unique signatures of X-ray ionization of the disks of low-mass YSOs.

Neon fine-structure lines have proved invaluable for studying ionized regions in our own as well as external galaxies (e.g., see the recent observations by Jaffe *et al.* 2003 of ultra compact H II regions in Monoceros R2, by Sturm *et al.* 2001 of AGN, by Devost *et al.* 2004 of the starburst galaxy NGC 253 and by Weedman *et al.* 2005 of Seyfert galaxies). The Ne ions in H II regions and galaxies are generated by the Lyman continuum photons from massive stars and by X-rays. Generating these ions with UV photons is much more difficult in the environment of low-mass young stellar objects. Cosmic rays are also unlikely to be effective for this purpose because they are excluded by the strong winds generated by YSOs (Glassgold, Najita & Igea 1997).

Low-mass YSOs are known to be strong emitters of moderately hard keV X-rays (e.g., Feigelson & Montmerle 1999), and we suggest that the Ne ions are mainly produced by X-rays. The basic idea is that the high ionization potentials of Ne and Ne^+ (21.56 and 41.0 eV, respectively) preclude the production of these ions by the FUV radiation ($\lambda > 911.6\,\mathrm{\AA}$) emitted by T Tauri stars. We will show that the hard X-rays emitted by YSOs are effective in generating Ne^+ and Ne^{2+} over a range of radii in the atmospheres of the disks of these stars. The emission arises in the same region of the disk from which photo-evaporation is believed to originate. Thus the Ne ion fine-structure line emission can serve as a diagnostic of the source of an evaporative flow as well as the signature of X-ray irradiation.

T Tauri stars are also likely to emit significant amounts of EUV radiation ($\lambda \lesssim 911.6\,\mathrm{\AA}$) (e.g., Alexander, Clarke and Pringle 2005), although it is much less well characterized than their X-ray emission. EUV radiation has been invoked to photo-evaporate disks (reviewed by

Hollenbach *et al.* 2000, Dullemond *et al.* 2006). However, EUV photons are rapidly absorbed by atomic hydrogen in the partially-ionized wind and disk of YSOs (Alexander, Clarke and Pringle 2003) so that, except for a fully-ionized region near the star (Hollenbach *et al.* 1994), the EUV flux that reaches substantial radii and depths in disks to generate Ne ions is probably very small. The small ionized region generated by stellar EUV radiation may be the source of some Ne fine-structure line emission (U. Gorti and D. Hollenbach, private communication 2006).

The plan of this article is as follows. First, we lay the foundation for calculating the fluxes of the X-ray generated Ne fine-structure emission by developing the ionization theory for the Ne ions. We take into account production by X-rays and destruction by charge exchange as well as radiative recombination in a form appropriate to the thermal-chemical structure of X-ray irradiated protoplanetary disk atmospheres. In §3, we calculate the fluxes of the fine-structure lines for the disk atmosphere of a typical T Tauri disk, where the electron densities are generally sub-critical. In §4 we discuss the observability of these lines, their potential astrophysical significance, and the uncertainties in the theory.

2. Ionization Theory

We start by discussing the production and destruction of Ne ions in the inner region of a protoplanetary disk atmosphere, within tens of AU. We consider only X-rays for ionizing the neutral and low-ionization forms of the Ne atom, since FUV photons have insufficient energy to ionize them, EUV is absorbed over short distances in mainly neutral matter, and cosmic rays are largely excluded from the inner regions, as mentioned in §1. Collisional ionization by thermal electrons is unimportant for the relevant temperatures, $T \lesssim 10,000\,\mathrm{K}$.

The result of an X-ray absorption by a low-ionized Ne ion depends on whether the X-ray energy E is less than or greater than the K-shell threshold, $E_K = 0.870, 0.903, \ldots$ keV for Ne I, Ne II $\ldots$. According to simple one-electron theory (e.g., Kaastra & Mewe 1993), an L-shell electron is ejected when $E < E_K$, increasing the ion charge by one. For $E > E_K$, the cross section for L-shell photoionization is small compared with the production of a K-shell vacancy, and the latter leads mainly to the ejection of another electron by the Auger process. According to one-electron theory (ignoring correlations), the branching ratio for single ionization is only 2% (Kaastra & Mewe 1993). The actual situation is more complicated, especially with regard to the production of more than two electrons, as was shown in laboratory experiments on neutral Ne by Carlson & Krause and collaborators (Krause *et al.* 1964; Carlson & Krause 1965a,b). First of all, there is a small but significant probability, $\sim 10\%$, that L-shell photoionization ejects *two* electrons. Second, the probability

that K-shell vacancies produce just one electron is somewhat larger ($\sim 6\%$) than predicted by one-electron theory ignoring electron correlations. Third, and most important, $\sim 30\%$ of K-shell vacancies produced in the photoionization of neutral Ne lead with significant probability to higher ions such as Ne^{3+} and Ne^{4+}. However, in partially-ionized regions characteristic of the atmospheres of protoplanetary disks , where atomic hydrogen is the dominant species in contrast to fully ionized H II regions, Ne^{3+} is rapidly destroyed by charge exchange with atomic hydrogen,

$$Ne^{3+} + H \rightarrow Ne^{2+} + H^{+}. \tag{2-1}$$

The cross section for this reaction has been measured to be large and rising down to 0.1 eV by Rejoub *et al.* (2004); it corresponds to rate coefficients for charge transfer $\sim 10^{-9}\,\mathrm{cm^3 s^{-1}}$. In essence, ions beyond Ne^{2+} that arise from K-shell vacancies in Ne atoms and low-ionization ions are rapidly converted back to Ne^{2+} by one or more charge transfers with atomic hydrogen.

Charge exchange with atomic hydrogen is also important in the ionization balance of Ne, Ne^{+} and Ne^{2+}. Charge transfer of Ne^{2+} to H was studied by Dalgarno and collaborators 25 years ago (Butler, Bender & Dalgarno 1979; Dalgarno, Butler & Heil 1980; Butler, Heil & Dalgarno 1980; Butler & Dalgarno 1980). Their conclusion was that the rate coefficient for this process is exceedingly small, but that *radiative* charge exchange takes place with rate coefficient $k_2 \approx 10^{-14}\mathrm{cm^3 s^{-1}}$. Although this is much smaller than the (essentially Langevin) rate coefficient for fast charge transfer ($\sim 10^{-9}\,\mathrm{cm^3 s^{-1}}$), it cannot be ignored in partially-ionized regions because its effect is the same order of magnitude as radiative recombination, $\propto x_{\rm e}\alpha_2$, where α_2 is the recombination rate coefficient for Ne^{2+} and $x_{\rm e}$ is the fractional ionization. There are no reports on charge transfer from Ne^{+} to H, but the potential energy curves calculated for this system by Pendergast, Heck and Hayes (1994) indicate that radiative charge exchange is highly forbidden (A. Dalgarno, private communication). We conclude that Ne^{+} is primarily destroyed by radiative recombination and, to a lesser extent, by X-ray photoionization into higher ions.

These considerations on Ne^{+} and Ne^{2+} charge transfer to H provide the basis for a simple set of steady-state ionization balance equations. The steady state assumption is justified by the high electron density in the region relevant for the emission of the fine-structure lines, typically $\sim 10^{5}\mathrm{cm^{-3}}$. At these high densities, the time scale for the slowest process, radiative recombination, is ~ 1 yr, the same order or less than the orbital time and, more important, significantly less than the accretion time scale. We denote the fraction of Ne in charge state n by x_n ($n = 0, 1, 2$). We express the difference between X-ray ionization below and above the Ne I K-edge by writing the total X-ray ionization rate as the sum of a soft and a hard component,

$$\zeta(n) = \zeta_s(n) + \zeta_h(n) \qquad\qquad (n = 0, 1). \tag{2-2}$$

Following the above discussion, we introduce branching ratios B_1 and B_2 for soft X-ray ionization of Ne to produce Ne^+ ($B_1 \approx 0.9$) and for hard X-ray ionization of Ne to produce Ne^{2+} ($B_2 \approx 0.94$, when fast charge exchange of higher ions back to Ne^{2+} is included). The steady balance equations for Ne^+ and Ne^{2+} are then:

$$\left[B_1\frac{\zeta_s(0)}{n_{\rm H}} + (1-B_2)\frac{\zeta_h(0)}{n_{\rm H}}\right] x_0 + (\alpha_2 x_{\rm e} + k_2)x_2 = \left[\frac{\zeta(1)}{n_{\rm H}} + (\alpha_1 x_{\rm e} + k_1)\right] x_1, \tag{2-3}$$

$$\left[(1-B_1)\frac{\zeta_s(0)}{n_{\rm H}} + B_2\frac{\zeta_h(0)}{n_{\rm H}}\right] x_0 + \frac{\zeta(1)}{n_{\rm H}}\, x_1 = (\alpha_2 x_{\rm e} + k_2)\, x_2, \tag{2-4}$$

where $n_{\rm H}$ is the number density of hydrogen nuclei. These equations can easily be solved in terms of the ion abundance ratios,

$$\frac{x_1}{x_0} = \frac{\zeta(0)/n_{\rm H}}{\alpha_1 x_{\rm e} + k_1}, \tag{2-5}$$

$$\frac{x_2}{x_0} = B_2\frac{\zeta_h(0)/n_{\rm H}}{\alpha_2 x_{\rm e} + k_2} + (1-B_1)\frac{\zeta_s(0)/n_{\rm H}}{\alpha_2 x_{\rm e} + k_2} + \frac{\zeta(1)/n_{\rm H}}{\alpha_2 x_{\rm e} + k_2}\,\frac{x_1}{x_0}, \tag{2-6}$$

with the proviso that $x_0 + x_1 + x_2 = x_{\rm Ne}$, where $x_{\rm Ne}$ is the disk abundance of gaseous Ne. When we recall from §2 that k_1 is negligible and ignore the small quantities $(1 - B_n)$ and the small difference between $\zeta(0)$ and $\zeta(1)$, we obtain the following relations:

$$\frac{x_1}{x_0} = \frac{\zeta({\rm Ne})/n_{\rm H}}{\alpha_1 x_{\rm e}}, \tag{2-7}$$

$$\frac{x_2}{x_0} = \frac{\zeta_h({\rm Ne})/n_{\rm H}}{\alpha_2 x_{\rm e} + k_2} + \frac{\zeta({\rm Ne})/n_{\rm H}}{\alpha_2 x_{\rm e} + k_2}\,\frac{x_1}{x_0}, \tag{2-8}$$

where $\zeta({\rm Ne}) = \zeta_s({\rm Ne}) + \zeta_h({\rm Ne})$ is the ionization rate for neutral Ne per Ne nucleus. The direct X-ray ionization rates for Ne can be calculated from the absorption cross section (Morrison & McCammon 1983; Wilms *et al.* 2000). Here we adopt an approximate treatment in which the Ne rates are scaled from ζ, the ionization rate per H nucleus, according to the ratio of the Ne cross section to the mean cross section that defines ζ. Following GNI04, we assume that the X-ray luminosity and spectral temperature are $L_{\rm bol} = 2 \times 10^{30}\,{\rm erg\,s^{-1}}$ and $kT_{\rm X} = 1\,{\rm keV}$, so that the X-ray spectrum extends from several hundred eV to a few KeV. Good representative figures before attenuation are $\zeta({\rm Ne}) \approx 40\zeta$ and $\zeta_h({\rm Ne})/\zeta({\rm Ne}) \approx 7/8$. These ratios are actually a function of position because the X-ray spectrum hardens due to the preferential absorption of soft X-rays. Thus the ratio $\zeta_h({\rm Ne})/\zeta({\rm Ne})$ tends to unity at large column density. The ratio $\zeta({\rm Ne})/\zeta$ is much greater than one because the X-rays emitted by young stellar objects have characteristic energies of the same order or larger than the Ne K-edge near 0.9 keV, where the Ne absorption cross section is maximum. In particular, the photoionization cross section of Ne for keV X-rays is much larger than the

cross section summed over a cosmic abundance mix (Morrison and McCammon 1983; Wilms *et al.* 2000) that determines ζ, the ionization rate per hydrogen nucleus. If the stellar X-ray spectrum contained few keV photons, the ratios $\zeta(\mathrm{Ne})/\zeta$ and $\zeta_h(\mathrm{Ne})/\zeta(\mathrm{Ne})$ would be very much smaller than the representative values quoted above. The secondary electrons generated by the primary photoionization can ionize hydrogen as well as a heavy element like Ne. But the electronic ionization cross section for Ne is generally no more than twice those for hydrogen and helium. Following the discussion of Maloney, Hollenbach & Tielens (1996), we estimate that the contribution of the secondary electrons to the X-ray ionization rate of Ne is $\lesssim 2\zeta$, and thus small compared to the direct X-ray ionization.

We will find in §3 that, for the regions of the disk responsible for the emission of the fine-structure lines, the fractions x_1/x_0 and x_2/x_0 are usually $\lesssim 0.1$ and thus

$$\frac{x_1}{x_0} = \frac{\zeta(\mathrm{Ne})/n_\mathrm{H}}{\alpha_1 x_\mathrm{e}} \equiv a_1, \qquad\qquad \frac{x_2}{x_0} \approx \frac{\zeta_h(\mathrm{Ne})/n_\mathrm{H}}{k_2 + \alpha_2\, x_\mathrm{e}} \equiv a_2. \tag{2-9}$$

Because $\alpha_2 > \alpha_1$ and k_2 is finite though small, these equations tell us that there is substantially more Ne^+ than Ne^{2+}.

Over most of the region of interest, the electron fraction is approximately given in terms of the total ionization rate by the simple formula,

$$x_\mathrm{e} \approx \left(\frac{\zeta}{n_\mathrm{H}\alpha(\mathrm{H}^+)}\right)^{1/2}, \tag{2-10}$$

where $\alpha(\mathrm{H}^+)$ is the total recombination rate of H^+. Therefore, according to equations 2-9 and 2-10, the fractions of Ne in the first two ion states depend on different powers of the ionization parameter ζ/n_H and, equivalently, the electron fraction,

$$\frac{x_1}{x_0} \sim (\zeta/n_\mathrm{H})^{1/2} \sim x_\mathrm{e}, \qquad\qquad \frac{x_2}{x_0} \sim \zeta/n_\mathrm{H} \sim x_\mathrm{e}^2. \tag{2-11}$$

The actual ionization fractions used in the calculations of §3 are,

$$x_0/x_\mathrm{Ne} = \frac{1}{d}, \qquad x_1/x_\mathrm{Ne} = \frac{a_1}{d}, \qquad x_2/x_\mathrm{Ne} = \frac{(a_1+b)a_2}{d}, \tag{2-12}$$

where $d = 1 + a_1 + (a_1 + b)a_2$ with $b \equiv \zeta_h(\mathrm{Ne})/\zeta(\mathrm{Ne}) \cong 0.875$.

In addition to their utility in the numerical calculations, these analytic formulae provide some insight into the physics of Neon ionization in X-ray irradiated protoplanetary disk atmospheres. In the first member of Eq. 2-11, the approximate proportionality of x_1/x_0 to the electron fraction is similar in form to the well known ratio of O^+ to O when O^+ and H^+ are strongly coupled by fast, near-resonant, charge exchange (e.g., Osterbrock 1987). In

the present case, Ne^+ and H^+ are not connected directly by charge exchange, but they are linked by both being produced by X-rays. A semi-quantitative expression of this relation, based on Eq. 2-11, is,

$$\frac{x(\mathrm{Ne}^+)}{x(\mathrm{Ne})} \sim \frac{\alpha(\mathrm{H}^+)}{\alpha_1}\,\frac{\zeta(\mathrm{Ne})}{\zeta}\,x_\mathrm{e}. \tag{2-13}$$

Because the ratio $\zeta(\mathrm{Ne})/\zeta \gg 1$ and α_1 is not very much smaller than $\alpha(\mathrm{H}^+)$, $x(\mathrm{Ne}^+)/x(\mathrm{Ne})$ is much larger than x_e. Although Eq. 2-13 expresses much of the essential physics of the X-ray ionization of Ne for protoplanetary disks, it is inadequate for quantitative estimates because it breaks down for very small and very large x_e.

In the next section, we use the detailed Ne ionization theory presented above to estimate the Ne ion line fluxes for a T-Tauri disk. We adopt, for this purpose, the thermal-chemical disk structure of an existing model that includes stellar X-ray heating and ionization (GNI04) but which did not include the Ne ionization theory discussed above. The GNI04 model allows for the inclusion of additional mechanical heating of the disk atmosphere, e.g., from accretion or wind-disk interaction, using the following formula for the volumetric heating rate

$$\Gamma_\mathrm{mech} = \frac{9}{4}\alpha_h \rho c^2 \Omega, \tag{2-14}$$

where α_h is a phenomenological parameter. Figure 1 is an example of the results of GNI04 at a radius of $R = 5\,\mathrm{AU}$; additional results for a range of radii are presented below in Figures 2 and 3. Figure 1 compares the vertical variation of the gas and dust temperatures. The abscissa represents the height above the midplane z in terms of the vertical column density N_H of hydrogen from ∞ down to z. The calculations are based on the D'Alessio *et al.* (1999) fiducial dust model for a T Tauri star with mass $M_* = 0.5 M_\odot$, radius $R_* = 2R_\odot$, and effective temperature $T_* = 4000\,\mathrm{K}$. The accretion rate is $\dot{M} = 10^{-8} M_\odot\ \mathrm{yr}^{-1}$, and the disk thickness at 1 AU is $\sim 100\ \mathrm{g\ cm^{-2}}$ and varies elsewhere roughly as $1/R$. Heating of small grains by the stellar optical and near infrared radiation produces an inversion in the dust temperature T_d over the midplane value, as shown by the dashed curve. X-ray heating generates a much larger inversion in the *gas* temperature T_g (solid line labeled $\alpha_h = 0.01$) in the region above the warm dust. When mechanical heating is included (the solid curve labeled $\alpha_h = 1.0$), the hot gas extends even further down into the disk. The gas and dust temperatures approach one another near the midplane (large N_H), where the volume densities n_H are big enough to ensure good thermal coupling between the gas and the dust. In between the hot gas layer at the top of the atmosphere and the relatively cool midplane region is a warm transition zone ($N_\mathrm{H} \gtrsim 10^{21}\mathrm{cm}^{-2}$) where $T_g \approx 500 - 2000\,\mathrm{K}$. Gas temperature inversions can also be obtained with UV heating of small grains and PAHs (Kamp & Dullemond 2005, Nomura & Millar 2005). Major chemical transitions occur between 10^{21} and $10^{22}\,\mathrm{cm}^{-2}$. Significant levels of

H_2 and full formation of CO occur near $N_{\rm H} \sim 1 - 2 \times 10^{21}{\rm cm}^{-2}$, and complete formation of H_2 is achieved at $N_{\rm H} = 8.5 \times 10^{21}\,{\rm cm}^{-2}$.

Figure 2 shows gas temperature profiles for radii ranging from $R = 1 - 40\,{\rm AU}$ for the case $\alpha_h = 0.01$. They exhibit a hot gas layer on top of a cool one, with temperatures generally decreasing with increasing radial distance. The temperature at the top of the atmosphere decreases with radius due to inverse square dilution of the stellar X-rays. The temperature near the midplane decreases with distance because the viscous heating in the D'Alessio model decreases. The results for the case where mechanical heating dominates are similar, except that the transition from hot to cold occurs deeper down in the atmosphere. Beyond $R = 20\,{\rm AU}$, there is a qualitative change in the temperature profiles in that the maximum temperature drops from several thousand to several hundred K. Figure 3 shows clearly how X-ray irradiation can warm disk atmospheres out to large radii of the order of tens of AU. It is also noteworthy that the near-midplane temperature at large radii can fall below the grain freeze-out temperature for many volatile species. Although the freeze-out process is omitted from our present chemical model, it does not affect the calculation of the Ne fine-structure emission, which arises from the upper atmosphere of the disk where the temperature is high and freeze-out does not occur. Regions where freeze-out can occur do not contribute to the emission because the upper levels of the transitions, with excitation temperatures $\sim 1000\,{\rm K}$, are difficult to excite with electron collisions at low temperatures.

Figure 3 shows that the electron fraction decreases smoothly at high altitudes. It then drops more rapidly to a level $x_{\rm e} \sim 10^{-4}{-}10^{-5}$, at a depth close to where T_g begins to approach T_d and near where carbon becomes almost fully associated into CO. Figure 3 demonstrates that stellar X-rays can generate substantial levels of ionization in disk atmospheres out to large radii. The variation in gas temperature and ionization in Figures 2 and 3 are directly relevant to the strength of the Ne line fluxes. Above the thermal-chemical transition, especially in the range near $N_{\rm H} = 10^{19}{-}10^{20}{\rm cm}^{-2}$, the warm ionized conditions are conducive to obtaining large Ne ion abundances and significant populations of the upper levels of the Ne II 12.81 μm and Ne III 15.55 μm transitions.

3. Flux Calculation

We estimate the emission from the Ne I and Ne II fine-structure lines from a face-on disk in the optically-thin approximation. The lines originate in magnetic dipole transitions from the Ne II doublet and the Ne III triplet, whose properties are given in Table 1.

Table 1: Ne Fine Structure Levels

Ion	$\lambda\,(\mu\mathrm{m})$	$J_u - J_l$	$T_{ul}(\mathrm{K})$	A_{ul} (s^{-1})	$T^{-1/2}n_{cr}(ul)$ (cm^{-3})	$A_{ul}h\nu_{ul}$ (erg s^{-1})
Ne^{+}	12.81	1/2-3/2	1122.8	8.59×10^{-3}	5.53×10^{3}	1.332×10^{-15}
Ne^{2+}	15.55	1-2	925.8	5.97×10^{-3}	3.94×10^{3}	7.629×10^{-16}
Ne^{2+}	36.02	0-1	399	1.15×10^{-3}	7.20×10^{2}	6.337×10^{-17}

The critical electron densities for the transitions ($n_{cr} = A_{ul}/k_{ul}$, where k_{ul} is the electronic collisional de-excitation rate coefficient) are taken from Mendoza (1983) and are given in the next to last column of Table 1. We assume that electronic collisions are more important than H collisions in exciting these fine-structure transitions.

We ignore the $J = 0 - 1$ 36.02 μm transition of Ne III, which is an order of magnitude weaker than the $J = 1 - 2$ 15.55 μm transition, and the very weak $0 - 2$ magnetic quadrupole transition (not listed in Table 1). The optically-thin approximation is valid because the emission comes from a surface layer with limited vertical column density $N_{\rm H} < 10^{22}\,{\rm cm}^{-2}$. Deeper regions ($N_{\rm H} > 10^{22}\,{\rm cm}^{-2}$) do not contribute because they are either insufficiently ionized or too cool for the transitions to be collisionally excited.

The flux in a transition $u \rightarrow l$ of an ion with charge n (the ion label $n = 1, 2$ now becomes a line label, $n = 1$ for the 12.81 and $n = 2$ for the 15.55 μm transition) from a disk annulus between R and $R + dR$ is,

$$dF_{ul}(R; n) = \frac{1}{4\pi d^2}\, 2\pi R dR \int_0^\infty dN\, P_u(n)\, x_n\, (A_{ul} h\nu_{ul})_n\,, \tag{3-1}$$

where $P_u(n)$ is the normalized population of the upper level, A_{ul} and $h\nu_{ul}$ are the usual A-value and energy of the transition, and $dN = dN_{\rm H}$ is the differential of the vertical hydrogen column density. At high densities, the populations are given by the Boltzmann distribution, whereas at low densities they reduce to the probability for a collisional excitation to occur within the radiative lifetime of the transition. In our calculations, the excited levels of the Ne fine-structure levels are populated near-thermally at $R = 1\,{\rm AU}$, but substantially sub-thermally at larger radii. The departure from a thermal population is conveniently expressed in terms of the factors,

$$\mathcal{C}_{ul} = 1 + \frac{n_{cr}(ul)}{n_{\rm e}}, \tag{3-2}$$

which make it possible to use Boltzmann-like formulae for the populations in this problem. Thus the population of the upper level of the Ne II 12.81 μm $J = 1/2 - 3/2$ transition is given by,

$$P_u(1) = \frac{1}{2\mathcal{C}_{3/2-1/2}\, e^{1122.8/T} + 1}, \tag{3-3}$$

and the population of the Ne III 15.55 μm is given by

$$P_u(2) = \frac{1}{1 + 5/3\,\mathcal{C}_{1-2}\, e^{925.3/T} + 1/3\,\mathcal{C}_{0-1}\, e^{-399/T}}. \tag{3-4}$$

Equation 3-4 is an approximation based on ignoring the weak quadrupolar transitions, both collisional and radiative, that connect the top $J = 0$ and the bottom $J = 2$ levels of the Ne III

fine-structure triplet. The factor $\mathcal{C}_{ul}$ is unity in the high-density limit (thermal population) and proportional to the electron density in the low-density (sub-thermal) limit where every exciting collision produces a fine structure photon.

The key factors in Equation 3-1 for the differential flux are the integrals,

$$N_u(R;1) = \int_0^\infty dN\, P_u(1)\, x_1 = x_{\rm Ne} \int_0^\infty dN\, P_u(1)\, \frac{a_1}{d}, \tag{3-5}$$

$$N_u(R;2) = \int_0^\infty dN\, P_u(2)\, x_2 = x_{\rm Ne} \int_0^\infty dN\, P_u(2)\, \frac{(a_1+b)a_2}{d}, \tag{3-6}$$

making use of Eq. 2-12; $N_u(R;1)$ and $N_u(R;2)$ are the column densities of excited Ne ions that emit the dominant fine-structure lines of Ne II and Ne III at radius R. Thus the radial distribution of the flux is given by,

$$dF_{ul}(n) = \frac{1}{4\pi d^2}\, (A_{ul} h\nu_{ul})_n\, 2\pi\, R N_u(R;n)\, dR, \tag{3-7}$$

where the numerical values of $A_{ul}h\nu_{ul}$ are given in the last column of Table 1.

In Figure 4 we plot $N_u(R;n)$, which determines the emissivity per unit area of the 12.81μm line of Ne^+ and the 15.55μm line of Ne^{2+} through Equation 3-7. Two extreme thermal models are shown, one for X-ray heating dominant ($\alpha_h = 0.01$) and the other for mechanical heating dominant ($\alpha_h = 1.0$). The emissivities are generally strongly peaked at very small radii where the upper levels are near-thermally excited. The effects of the central peaking is suppressed somewhat due to the factor R in Equation 3-7 for the flux.

At larger radii, the excitation is sub-thermal, and the emissivities are determined by the second and third powers of the electron density, as suggested by Equation 2-11. The electron density profiles decrease in magnitude roughly as the inverse square of the radial distance. For large R, the emissivity is further reduced by the impact of the decrease of both $n_{\rm e}$ and T for large column densities. The emissivity of the 15.55μm line is smaller because of the reduced abundance of Ne^{2+}, due in large part to its destruction by charge exchange with atomic hydrogen. In addition, the characteristic quantity $(A_{ul}h\nu_{ul})_n$ is smaller by a factor of 1.75 for this transition compared to the 12.81μm line. The 12.81μm line of Ne^+ is more sensitive to the heating model because it tends to be emitted deeper in the atmosphere where mechanical heating can extend the warm temperature transition region.

The unresolved line fluxes can be obtained by integrating the emissivities in Figure 4 over radius, including the extra factor of R in Equation 3-7. The results are given in Table 2, assuming a nominal distance for the model T-Tauri star of $d = 140\,$pc and a Ne abundance of 10^{-4}. Approximately half of the flux of the 12.81μm line of Ne^+ arises from within 6 AU, with the remaining half produced over the radial range $6 - 30\,$AU.

Table 2: Neon Ion Line Fluxes (erg s^{-1} cm^{-2})

α_h	Ne^+ 12.81 μm	Ne^{2+} 15.55 μm
1.00	1.25×10^{-14}	6.46×10^{-16}
0.01	6.22×10^{-15}	5.27×10^{-16}

The flux of the 12.81 μm line for the two extreme heating models differs by only a factor of two, so we conclude that a typical T Tauri star generates a flux of $\sim 10^{-14}$erg cm^{-2}s^{-1}; the flux of the 15.55 μm line is about 20 times smaller, $\sim 5 \times 10^{-16}$erg cm^{-2}s^{-1}. The predicted value of the flux of the 12.81 μm line suggests that it may be observable with only moderate spectral resolution. The dust continuum emission for the D'Alessio generic T-Tauri star (at 140 pc) near 13μm is 1.21×10^{-11} erg s^{-1} cm^{-2} μm^{-1}. If we consider the *Spitzer* Infrared Spectrometer (IRS), with a spectral resolution of 600, the continuum flux within a spectral resolution element is 2.58×10^{-13} erg s^{-1} cm^{-2}, about 25 times larger than the theoretically predicted line flux. Thus a high signal-to-noise observation with the IRS should lead to a detection of the 12.81 μm line. The Ne^{2+} 15.55 μm line would be much more difficult to detect. These lines would become easier to detect in sources with weaker continua or with observations made at higher spectral resolution. Because H atom collisions have been ignored, the fluxes in Table 1 should be considered as lower limits.

This discussion of the observability of the Ne fine-structure lines has been based on a neon abundance of 10^{-4}, or equivalently on a solar abundance ratio of neon to oxygen, Ne/O = 1/6. Several lines of evidence have suggested that the Ne abundance is closer to $x_{\rm Ne} = 2.5 \times 10^{-4}$. *Chandra* X-ray spectroscopy of nearby stars with a wide range of the ratio $L_{\rm bol}/L_{\rm X}$ give a nearly constant Ne/O = 0.4 (Drake & Testa 2005). For the few T Tauri stars where the same measurements have been made, two are in harmony with this result (BP Tau and TWA 5 with Ne/O $\approx$ 0.5) and one has an even larger value (TW Hya with Ne/O = 0.87 ± 0.13), as discussed by Drake, Testa & Hartmann (2005). Measurements of Orion B stars also give a larger Ne abundance than 10^{-4}, $x_{\rm Ne} = 1.29 \times 10^{-4}$ and a larger neon to oxygen ratio, Ne/O = 0.25 (Cunha, Hubeny & Lanz 2006). The solar Ne abundance plays a key role in the continuing controversy between the results of helio-seismology and solar models (Asplund *et al.* 2004, Antia & Basu 2005, Bahcall, Basu & Serenelli 2005, Schmelz *et al.* 2005, Delahaye & Pinsonneault 2006). Despite these uncertainties, our results suggest that disk Ne abundances anywhere in the above range of values are sufficient to produce detectable Ne^{+} emission.

The spatial distribution of the emissivity in Figures 4 has consequences for the rotational broadening of the Ne fine structure lines emitted by protoplanetary disks. Assuming Keplerian rotation, the column density $N_u(R;n)$ can be converted into a distribution function $P(v)$ for the rotational speed ($P(v)dv \propto N_u(R)R\,dR$) such that $P(v)dv$ is the fraction of emission within the speed interval dv,

$$P(v) \propto v^{-5} N_u(R(v);n) \tag{3-8}$$

where $R = GM_*v^{-2}$. When combined suitably with the distribution of turbulent velocities, $P(v)$ helps determine the shape of the lines. Figure 5 shows the distribution function $P(v)$

for the Ne II 12.81 μm line, where the abscissa is $w = v/v(1\,\mathrm{AU}) > 0$. We see that $P(v)$ has two components. One is a narrow distribution centered at $0.25\,v(1\,\mathrm{AU})$, which corresponds to the cut-off of the spatial variation of $N_u(R;n)$ in Figure 4 beyond 16 AU. Then there is a long tail extending to the maximum rotational speed, which arises from the peaking of the spatial distributions in Figure 4 at small R. Ignoring turbulent broadening, the rotational lineshape function for inclined disks will have a double peak, associated with the cut-off of the emissivity at large radii, plus extended line wings associated with the concentration of the emission at small radii. In principle, this analysis can be used to obtain information about the spatial distribution of the emission from measurements of the lineshape. Assuming that the turbulent velocities are of order $1\,\mathrm{km\,s^{-1}}$, as suggested by the measured CO lineshapes of T Tauri stars (Najita *et al.* 2006), moderately-high spectral resolution observations with $R \sim 3 \times 10^4$ could confirm the expectations for the Ne lineshapes based on Figure 5.

4. Discussion

In the last section, we concluded that the Ne^+ 12.81μm line should be detectable from a typical T Tauri star with a moderate resolution spectrometer like the *Spitzer* IRS. Indeed. we have reports from colleagues of the detection with this instrument of unusually strong 12.81μm emission from a few T Tauri stars (Ilaria Pascucci 2006, Dan Watson 2006 private communications). These are probably the brightest Ne fine-structure emission line sources; the emission from most others is likely to be fainter. This line is also observable from the ground, and attempts to observe it with a large telescope at high spectral resolution would be of great interest. Not only would the line to continuum ratio be increased, but it might become possible to obtain information about the line shape, as discussed at the end of §3, that would help locate the source of the emission in the disk.

We have argued that the detection of the Ne ion fine-structure lines would provide clear support for the role of stellar X-rays in determining the physical properties of the atmosphere of YSO disks, the region most accessible to observational study. The Ne lines complement the detection of the ro-vibrational transitions of CO and the UV fluorescence of H_2 (reviewed by Najita *et al.* 2006). The latter transitions are associated with material at disk radii within a few AU and with vertical column densities $N_\mathrm{H} \gtrsim 10^{21}\mathrm{cm}^{-2}$. Our calculations show that the emission of the Ne fine structure lines arises from a larger range of radial distances, out to $10 - 15\,\mathrm{AU}$, and that the lines are formed mainly at vertical column densities in the range $N_\mathrm{H} \sim 10^{19} - 10^{20}\mathrm{cm}^{-2}$. Thus the Ne fine-structure transitions are complementary to the lines of CO and H_2 in probing both the warm temperature region above the cool molecular layer and a region that extends to relatively large radii that, in our own solar system, would

range from the location of the terrestrial planets to beyond the giant planets. By contrast, both the UV transitions of H_2 and the CO ro-vibrational transitions are generally restricted to the inner few AU of disks (Najita *et al.* 2003; Najita *et al.* 2006), and the IR transitions of H_2 are likely to probe a narrow range of radii (Pascucci *et al.* 2006).

The measurement of Ne lines in the disks of low-mass YSOs is also of interest because of the special chemistry of neon. From the disk modeling perspective, Ne has the advantage that the complexities of molecule formation and destruction do not enter. It is unlikely that significant amounts of Ne will freeze out on dust grains, although some of the neon trapped in meteorites has been interpreted in terms of adsorption (e.g., Swindle 1988). Thus the detection of the Ne fine-structure lines, in conjunction with model calculations, might eventually provide information on the abundance of Ne in YSO disks, which serve as observable analogs of the primitive solar nebula. Because the Ne lines arise in a relatively thin layer at high altitudes, by themselves they provide only weak constraints on the total gas mass of protoplanetary disks. However, when taken together with other diagnostics, such as CO and H_2, detailed modeling of several species might provide important information on disk gas mass.

The calculations reported in this paper are limited to the fine-structure lines of just one element and one type of disk, the typical T Tauri disk as formulated by D'Alessio *et al.* (1999). In addition to extending the range of application of models such as ours (see also the work of Gorti & Hollenbach 2004), attention needs to be given to the underlying physics and chemistry of disk modeling, some of which is quite uncertain and affects the accuracy of model predictions.

The emission of Ne fine-structure lines from relatively cool YSO disks arises from the ejection by hard X-rays of the K-shell electrons of moderately heavy ions, followed by the Auger effect. This process is enhanced as the mass of the target ion is increased, and it surely occurs for other abundant elements such as Si, S, and Fe. Our analysis of Ne fine-structure lines shows how important the recombination cascade from higher to lower ion stages is in determining the abundance of the first few (and most abundant) ions. Sulfur serves as a good example. Gorti and Hollenbach (2004) and Hollenbach *et al.* (2005) have suggested that the S I 25.2 and 56.3 μm fine-structure lines, among others, are potential diagnostics of intermediate-age YSO disks. Hard X-rays will produce ions as high as S^{6+}, and the highest ions are expected to be destroyed by a chain of fast charge transfers with atomic hydrogen, as has been confirmed by a high-level theoretical calculation by Stancil *et al.* (2001) of the reaction $S^{4+} + H \rightarrow S^{3+} + H^+$, which is fast down to low energies. However, the situation for S^{3+} and S^{2+} remains problematic. Early calculations of $S^{2+} + H \rightarrow S^+ + H^+$ (Butler & Dalgarno 1980, Christensen & Watson 1981) suggest that the rate coefficient is small at

low temperatures. Recent calculations of S^{3+} charge exchange (Bacchus-Montabonel 1998; Labuda *et al.* 2004) are restricted to keV energies. The recent study of the reaction, $H^+ + S \rightarrow S^+ + H$, by Zhao *et al.* (2005) provides important information for the ionization balance between S and S^+, but theoretical and experimental studies of S^{2+} and S^{3+} charge transfer with H at low energies ($\lesssim 1\,\mathrm{eV}$) are needed before the emission of the S I and S III fine-structure lines can be calculated reliably for X-ray irradiated disks, e.g., along the lines of the analysis for neon in this paper. A similar conclusion applies to other heavy elements for which low-energy charge-transfer cross sections with H are lacking for the first few ions.

It is important to recall the discussion of low-energy Ne ion charge exchange in §2. In particular, we have relied on 25 year old theoretical estimates in adopting a rate coefficient $k_2 = 10^{-14}\mathrm{cm^3 s^{-1}}$ for the charge transfer from Ne^{2+} to H. Because the detectability of the Ne III 15.55 μm line depends on this coefficient, it would be important to have more theoretical work on this reaction. We also have no information on the rate coefficients for the excitation of the Ne ion fine-structure levels by atomic hydrogen. Although few in number, existing calculations (e.g., Launay & Roueff 1977 & Barinovs et al. 2005 for H + C^+) lead to rates $\sim 10^{-9}\mathrm{cm^3 s^{-1}}$. If this order of magnitude is appropriate for the Ne ions, then H atom collisions would be important in that part of the disk atmosphere where $x_\mathrm{e} < 0.01$ and T is still large enough to excite levels with excitation temperatures of order 1000 K. Our flux estimates may also be affected by the lack of understanding of other basic microscopic processes, not to mention the many astrophysical uncertainties such as disk structure, dynamics and thermodynamics. We have considered the possibility that the Ne ions are destroyed by molecules and PAHs. It is known from room temperature experiments (Anicich 1993) that Ne^+ does not react strongly if at all with H_2 and CO, molecules that are predicted to occur at reduced levels in the warm upper atmosphere. Depending on their charge and abundance, PAHs might conceivably pay a role in destroying Ne ions and thus reduce the strength of the fine-structure lines. Negatively charged PAHs can neutralize Ne ions with large reaction rate coefficients (e.g., Tielens 2005). Both capture and charge transfer are possible reactions with neutral PAHs. Using rate coefficient estimates in the literature (Bohme 1992, Tielens 2005) and a maximal PAH abundance of 10^{-7}, we find that these neutral reactions are less important than destruction by radiative recombination. Of course, there is also the strong possibility that the PAH abundance in YSO disk atmospheres is reduced by the strong stellar X-ray flux or by the ions that the X-rays generate. It would appear that the largest uncertainty in the underlying microphysics of our analysis of the neon ion abundances and their fine-structure line emission is in the magnitude of the weak but not insignificant charge transfer to atomic hydrogen.

One astrophysical uncertainty that affects our estimates of the line fluxes is the GNI04 choice of the X-ray luminosity and spectral temperature, $L_\mathrm{bol} = 2 \times 10^{30}\,\mathrm{erg\,s^{-1}}$ and $kT_\mathrm{X} =$

1 keV. The former is characteristic of solar-like YSOs observed by *Chandra* in the Orion Nebula Cluster (Garmire *et al.*. 2000, Wolk *et al.* 2005). This may well be an overestimate for the X-ray luminosity of lower-mass and older T Tauri stars. Based again on *Chandra* observations of the Orion Nebula Cluster (Preibisch *et al.* 2005), the X-ray luminosity is measured to be smaller for lower-mass and older YSOs, and it is suppressed somewhat for accreting as opposed to non-accreting systems. Rather than use just a single temperature, it would be more appropriate to represent the X-ray spectrum with a two-temperature model of the type used to fit X-ray observations of well-observed stars. More generally, in future modeling of specific stars, the observed X-ray spectra should be used.

We can use the approximations developed in §2, especially Equations 2-10 and 2-11, to identify some of the other astrophysical uncertainties in our flux estimates. The Ne levels are sub-thermally excited over most of the disk volume responsible for the emission of the fine-structure lines. Thus the local emissivity of the Ne II 12.81 μm line is determined by $n_{\rm e}^2$, because the Ne^+ abundance usually tracks the electron fraction (Eq. 2-11). Equation 2-10 now tells us that the emissivity is determined roughly by

$$j(\mathrm{Ne}^+) \propto x_{\rm Ne}\, n_{\rm H}\, \zeta(\mathrm{Ne})\, \frac{k_{lu}(T)}{\alpha_1(T)}, \tag{4-1}$$

i.e., by the product of the Ne abundance, the local density, the ionization rate (including attenuation), and a function of temperature that is essentially the Boltzmann factor, $\exp\left(-T_{ul}/T\right)$. This last factor is one of several responsible for cutting off the emissivity at large column densities (and large radii). Equation 4-1 suggests that the Ne II 12.81 μm line strength will be larger for younger and more active T Tauri stars, which have larger densities and ionization rates. However, this does not mean that the line will be easier to detect from such stars, because their dust continuum emission will also be larger.

Flaring of the disk also plays a role in that the more flaring the smaller the attenuation of the X-rays. The GNI04 is flawed in this respect because it uses the D'Alessio *et al.* (1999) density distribution, whose scale height is determined by the dust temperature. In a thermal-chemical model that treats hydrostatic equilibrium self-consistently, we would expect an even more diffuse atmosphere than the one used in this paper. Furthermore, Table 2 shows that, without mechanical heating, the flux Ne II 12.81 μm line is reduced by a factor of two. In other words, the emissivity is affected by the poorly understood processes that heat the disk atmosphere. Clearly, there are many possibilities for variation of the Ne fine-structure line fluxes, and some if not many T Tauri stars may generate fluxes smaller than those given in Table 2.

In conclusion, we have modeled the physical properties of the disk atmosphere of a generic T Tauri star exposed to a strong stellar X-ray flux, and we have calculated the abun-

dance of Ne^+ and Ne^{2+} and the strength of their fine-structure lines. The estimated fluxes indicate that the Ne II 12.81 μm line should be detectable with existing instrumentation. The observation of this line from warm disk atmospheres would provide strong evidence for the significant role of stellar X-rays on the physical and chemical properties of YSO disks and on the conditions for photoevaporation.

The authors would like to thank Alex Dalgarno for advice on neon ion charge transfer reactions with atomic hydrogen, Phil Stancil for information about sulfur ion charge exchange, Jack Lissauer for discussions on the potential role of neon in determining the gas mass of protoplanetary disks (a key quantity for the formation of the jovian planets) and David Hollenbach for discussing the possible role of EUV radiation in generating Ne ions and especially for his many helpful comments on this manuscript. This research has been supported by grants from NSF and the NASA Origins Program.

REFERENCES

Aikawa, Y. & Herbst, E. 1999, A&A, 351, 233

Alexander, R. D., Clarke, C. J. & Pringle, J. E. 2003, MNRAS, 348, 879

Alexander, R. D., Clarke, C. J. & Pringle, J. E. 2004, MNRAS, 354, 74

Alexander, R. D., Clarke, C. J. & Pringle, J. E. 2005, MNRAS, 358, 283

Anicich, V. G. 1993, ApJS, 84, 215

Asplund, M., Grevasse, N., Sauval, A. J., Allende Prieto, C. & Kiselman, D. 2004, A&A, 417, 751

Bacchus-Montabonel, M.-C. 1998, Chem. Phys. 228, 181

Bahcall, J. N., Basu, S. & Serenelli, A. M. 2005, ApJ, 631, 1281

Barinovs, G., van Hemert, M. C., Krems, R. Dalgarno, A. 2005, ApJ, 620, 537

Bohme, D. 1992, Chem. Rev. 92, 1487

Butler, S., Bender, C. F. & Dalgarno, A. 1980, ApJ, 230, L59

Butler, S., Heil. T. G. & Dalgarno, A. 1980, ApJ, 241, 442

Butler, S. & Dalgarno, A. 1980, ApJ, 241, 838

Carlson, T. A. & Krause, M. O. 1965a, Phys. Rev. Letts., 14, 390

Carlson, T. A. & Krause, M. O. 1965b, Phys. Rev., 140, A1057

Christensen & Watson, W. D. 1981, Phys. Rev. A24, 1331

Cunha, K., Hubeny, I., & Lanz, T. 2006, ApJ, 647, L143

Dalgarno, A. 1976, in *Atomic Processes and Applications*, eds. P. G. Burke & B. L. Moseiwitsch (North-Holland), p. 109

Dalgarno, A., Butler, S. E. & Heil. T. G. 1980, A&A, 89, 379

D'Alessio, P., Calvet, N., Hartmann, L., Lizano, S. & Cantó, J. 199, ApJ, 527, 893

Delahaye, F. & Pinsonneault, M. H. 2006, ApJ, 649, 529

Devost, D. *et al.*, 2004, ApJS, 154, 242

Dulllemond, C. P., Hollenbach, D., Kamp, I. & D'Alessio, P. D. 2006, in *Protostars and Planets V*, ed. B. Reipurth, (ASP:San Francisco), in press 2006

Draine, B. T. & Woods, D. T. 1989, ApJ, 363, 464

Drake, J. J. & Testa, P. 2005, Nature, 485, 525

Drake, J. J., Testa, P. & Hartmann, L. 2005, ApJ, 627, L149

Feigelson, E. D. & Montmerle, T. 1999, ARA&A, 37, 363

Garmire, G. *et al.* 2000, AJ. 120, 1426

Glassgold, A. E., Najita, J. & Igea, J. 1997, ApJ, 480, 344 (erratum, 485, 820)

Glassgold, A. E., Feigelson, E. D. & Montmerle, T. 2000, in *Protostars and Planets IV*, eds. V. Mannings, A. P. Boss, & S. S. Russell, (Tucson:Univ. Arizona Press), p. 429

Glassgold, A. E., Najita, J. & Igea, J. 2004, ApJ, 615, 972 (GNI04)

Gorti, U. & Hollenbach, D. J. 2004, ApJ, 613, 242

Gredel, R. & Dalgarno, A. 1995, ApJ, 446, 852

Halpern, J. & Grindlay, J. E. 1980, ApJ, 242, 1041

Herczeg, G. J., Linsky, J. L., Valenti, J. A., Johns-Krull, C. M. & Wood, B. E. 2002, ApJ, 572, 310

Hollenbach. D. J., Yorke, H. W. & Johnstone, D. 2000, in *Protostars and Planets IV*, eds. V. Mannings, A. P. Boss, & S. S. Russell, (Tucson:Univ. Arizona Press), p. 401

Hollenbach, D. J., Johnstone, D., Lizano, S. & Shu, F. H. 2004, ApJ, 428, 654

Hollenbach, D. J., Gorti, U., Meyer, M. *et al.* 2005, ApJ, 613, 424

Jaffe, D. T., Zhu, Q., Lacy, J. H. & Richter, M. 2003, ApJ, 596, 1063

Kamp, I. & , Dulllemond C. P. 2004, ApJ, 615, 991

Kaastra, J. S. & Mewe, R. 1993, A&AS, 97, 443

Krause, M. O., Vestal, M. L., Johnston, W. H., & Carlson, T. A. 1965, Phys. Rev. 133, A385

Krolik, J. H. & Kallman, T. R. 1983, ApJ, 267, 610

Labuda, M., Tergiman, Y. S., Bacchus-Montabonel, M.-C. & Sienkiewicz, J. E. 2004, Chem. Phys. Letts. 394, 446

Langer, W. D. 1978, ApJ, 225, 860

Launay, J.-M. & Roueff, E. 1977, J. Phys. B, 10, 879

Lepp, S. & McCray, R. 1983, ApJ, 269, 560

Lepp, S. & Dalgarno, A. 1996, A&A, 306, L21

Maloney, P. R., Hollenbach, D. J. & Tielens, A. G. G. M. 1996, ApJ, 466, 561

Markwick, A., Ilgner, M., Millar, T. J. & Henning, Th. 2004, A&A, 385, 642

Mendoza, C. 1983, in *Planetary Nebulae*, (Dordrecht:Reidel), p. 143

Morrison R. & McCammon, D. 1983, ApJ, 270, 119

Najita, J., Carr, J. S. & Mathieu, R. D. 2003, ApJ, 589, 931

Najita, J. R., Carr, J. S., Glassgold, A. E. & Valenti, J. A. 2006, in *Protostars and Planets V*, ed. B. Reipurth, (ASP:San Francisco), in press

Neufeld, D. A., Maloney, P. R. & Conger, S. 1994, ApJ, 435, L127

Nomura, H. & Millar, T. J. 2005, A&A, 438, 923

Osterbrock, D. E. 1989, *Astrophyics of Gaseous Nebulae and Actuve Galactic Nuclei*, (Mill Valley:University Science)

Pascucci, I., Gorti, U., Hollenbach, D. J. *et al.* 2006, astro-ph/0606669

Pendergast, P., Heck, J. M. & Hayes, E. F. 1994, Int. J. Qunantum Chemistry, 49, 405

Preibisch, T., Kim, Y.-C., Favata, F. *et al.* 2005, ApJS, 160, 401

Pudritz, R. E. & Silk, J. 1987, ApJ, 316, 213

Rejoub, R., Bannister, M. E., Savin, D. W. *et al.* 2004, Phys. Rev., A69, 052724

Silk, J. & Norman, C. 1983, ApJ, 272, L49

Schmelz, J. T., Nasraoui, J. K., Lippner, L. A., Garst, J. W. 2005, ApJ, 634, L197

Stancil. P. C., Turner, A. R., Cooper, D. L., Schultz, D. R., Raković, M. J., Fritsch, W. & Zygelman, B. 2001, J. Phys. B 34. 2481

Stäuber, P., Doty, S. D., van Dishoeck, E. F. & Benz, A. O. 2005, A&A, 440, 949

Sternberg, A., Yan, M. & Dalgarno, A. 1997, IAU Symposium 178, 141

Sturm, E., Lutz, D. & Verma, A. 2002, A&A, 393, 821

Swindle, T. D. 1988, in *Meteorites and the Early Solar System*, eds. J. F. Kerridge & M. S. Matthews, (Arizona:Tuscon), p. 535

Tielens, A. G. G. M. 2005, The Physics and Chemistry of the Interstellar Medium, (Cambridge: Cambridge), Ch. 6

Tiné, S., Lepp, S., Gredel, R. & Dalgarno, A. 1997, ApJ, 481, 282

Tsujimoto, M. *et al.* 2005, ApJS, 160, 503

Weedman, D. W., Hao, L., Higdon, S. J. U. *et al.* 2005, ApJ, 633, 706

Wilms, J., Allen, A. & McCray, R. 2000, ApJ, 542, 914

Wolk, S., Harnden, F. R. Jr., Flaccomio, E. *et al.* 2005, ApJS, 160, 423

Yan, M. & Dalgarno, A. 1997, ApJ, 481, 296

Zhao, L. B., Stancil, P. C., Gu, J.-P., Liebermann, H.-P., Funke, P., Buenker, R. J. & Kimura, M. 2005. Phys. Rev. A71, 1

Fig. 1.— Temperature profiles for a protoplanetary disk atmosphere based on GNI04. The radial distance is 5 AU, and the mass accretion rate is $10^{-8} M_\odot$ yr^{-1}. The abscissa is vertical column density in cm^{-2}, and the ordinate is temperature in degrees K. The lower dashed line is the dust temperature for the D'Alessio et al. (1999) generic T Tauri star model. The upper solid curves are gas temperature labeled by the phenomenological mechanical surface heating parameter defined by Equation 2-14: $\alpha_h = 1$ (mechanical heating dominant) and $\alpha_h = 0.01$ (X-ray heating dominant). The major chemical transitions occur between 10^{21} and 10^{22} cm^{-2}: significant levels of H_2 and full formation of CO occur near $N_{\rm H} \sim 1-2\times10^{21}$cm^{-2}, and complete formation of H_2 is achieved at $N_{\rm H} = 8.5 \times 10^{21}$ cm^{-2}.

Fig. 2.— Gas temperature profiles for the GNI04 disk atmosphere model for the case $\alpha_h = 0.01$. The abscissa is vertical column density in cm^{-2}, and the ordinate is temperature in degrees K. The general structure consists of a thin hot layer on top of a thick cool layer (near the midplane), with a warm transition layer in between.

Fig. 3.— Electron fractions for the GNI04 X-ray irradiated disk atmosphere model for the case $\alpha_h = 0.01$. The abscissa is vertical column density in cm^{-2}, and the ordinate is $x_{\rm e}$, the electron abundance relative to total hydrogen. Deeper down than a vertical column $N_{\rm H} = 3 \times 10^{20}$cm^{-2}, the electron fraction is $\lesssim 10^{-4}$.

Fig. 4.— The Ne fine-structure line emissivity per unit area, expressed in terms of column densities of the upper level from Equation 3-7, calculated with the GNI04 disk atmosphere model for a neon abundance of $x_{\rm Ne} = 10^{-4}$. There is a pair of curves for each fine-structure transition, Ne II 12.81μm and Ne III 15.55μm. The upper curve is for $\alpha_h = 1$ (mechanical heating dominant), and the lower curve is for $\alpha = 0.01$ (X-ray heating dominant). The emissivity is peaked at small R, and then drops off rapidly beyond $R \sim 16$ AU.

Fig. 5.— The distribution of rotational speeds of the Ne II 12.81 μm line emission. The abscissa is speed, normalized to the value at 1 AU (the smallest radius used in the present emissivity calculation), and the ordinate is the unnormalized probability. The peak is located near $0.25\, v(1{\rm AU})$, corresponding to the large-R cut-off in Figure 4. The long tail at large velocities is associated with the strong emission at small radii. This distribution, convolved with the distribution of turbulent velocities, determines the line shape, which will be double-peaked and exhibit substantial line wings for inclined disks.

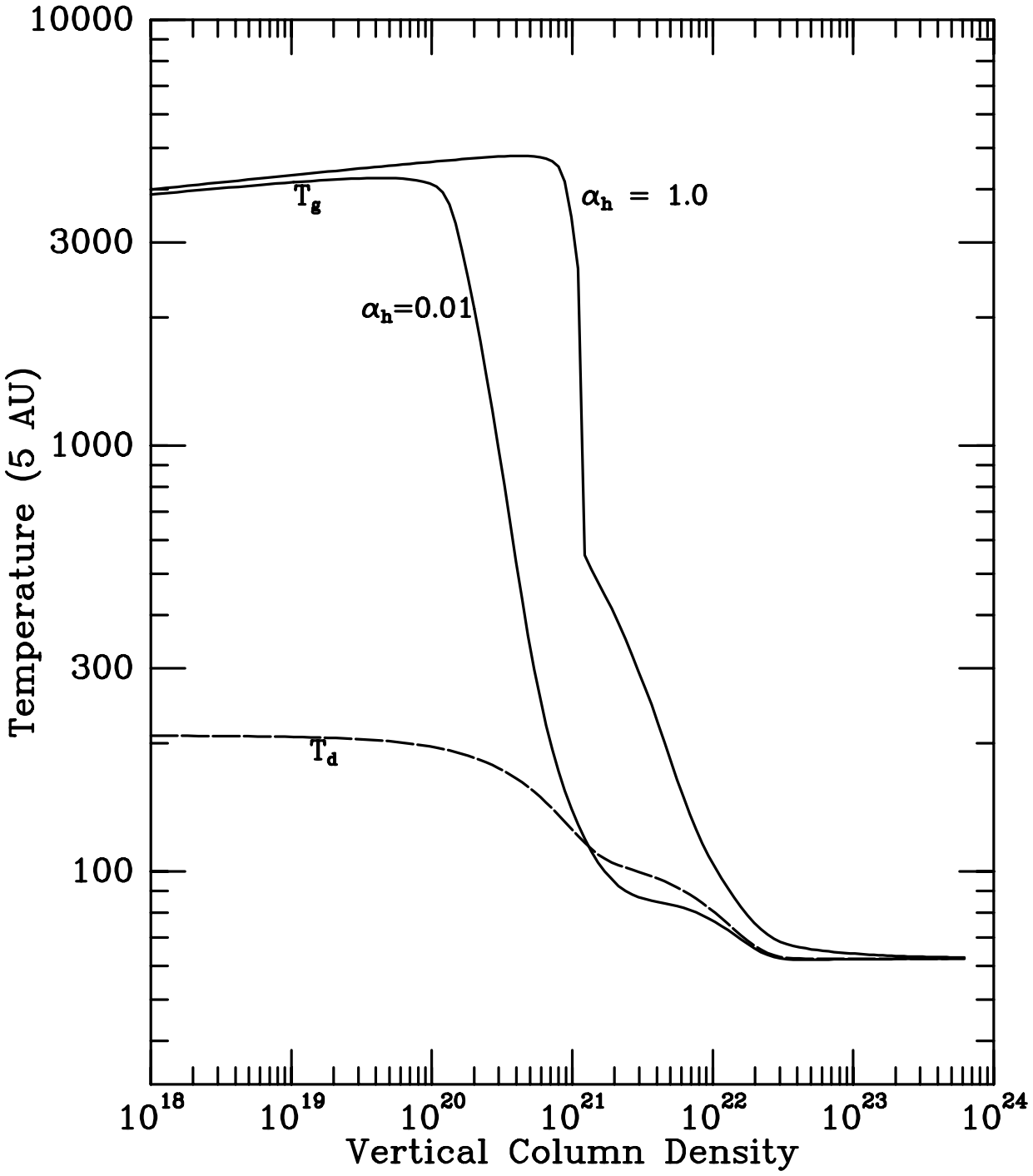
10000
3000
1000
300
100
Temperature (5 AU)
T_g
T_d
α_h = 1.0
α_h=0.01
10^{18}
10^{19}
10^{20}
10^{21}
10^{22}
10^{23}
10^{24}
Vertical Column Density

f1.eps

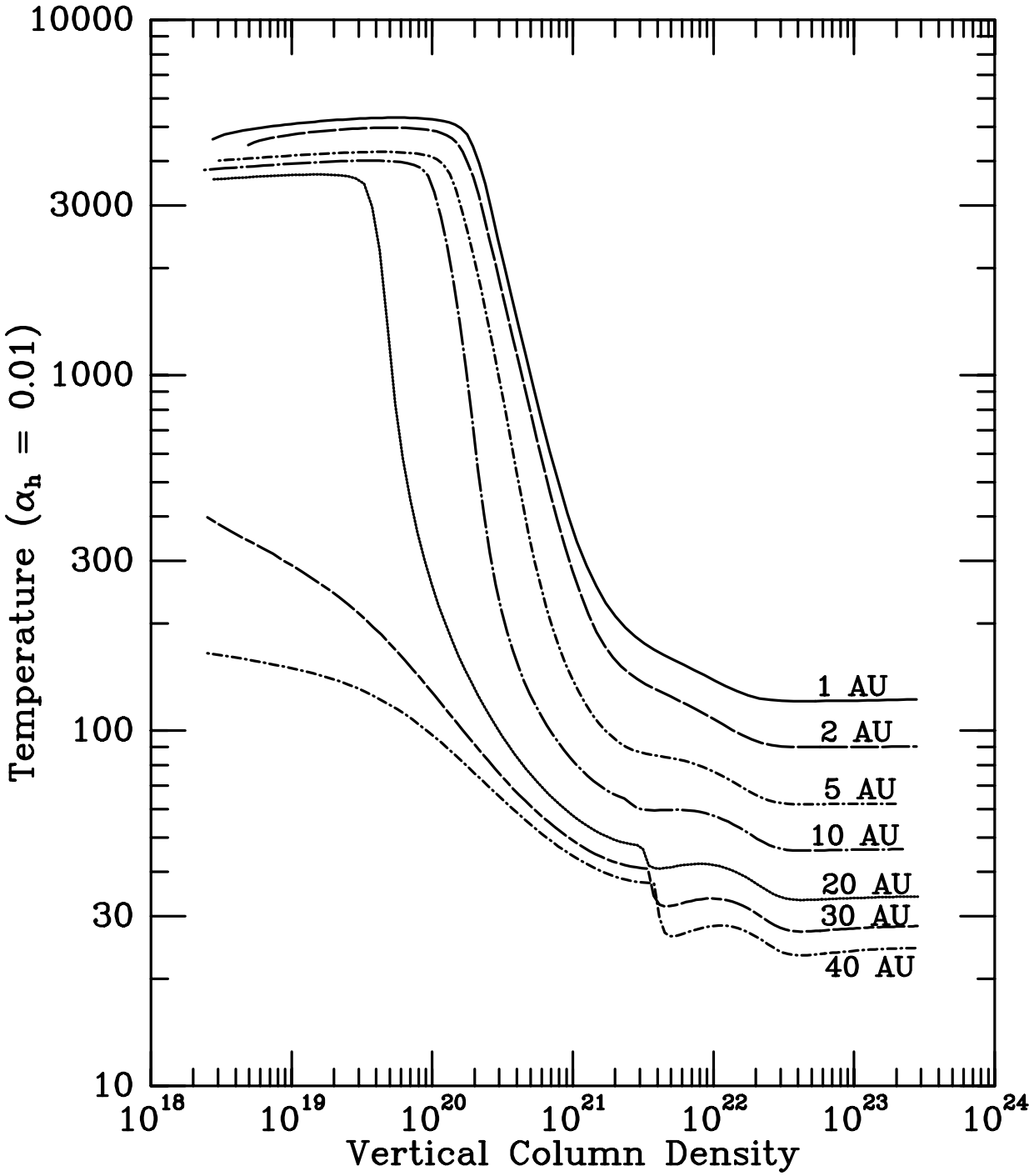
10000
3000
1000
300
100
30
10
Temperature (α_h = 0.01)
10^{18}
10^{19}
10^{20}
10^{21}
10^{22}
10^{23}
10^{24}
Vertical Column Density
1 AU
2 AU
5 AU
10 AU
20 AU
30 AU
40 AU

f2.eps

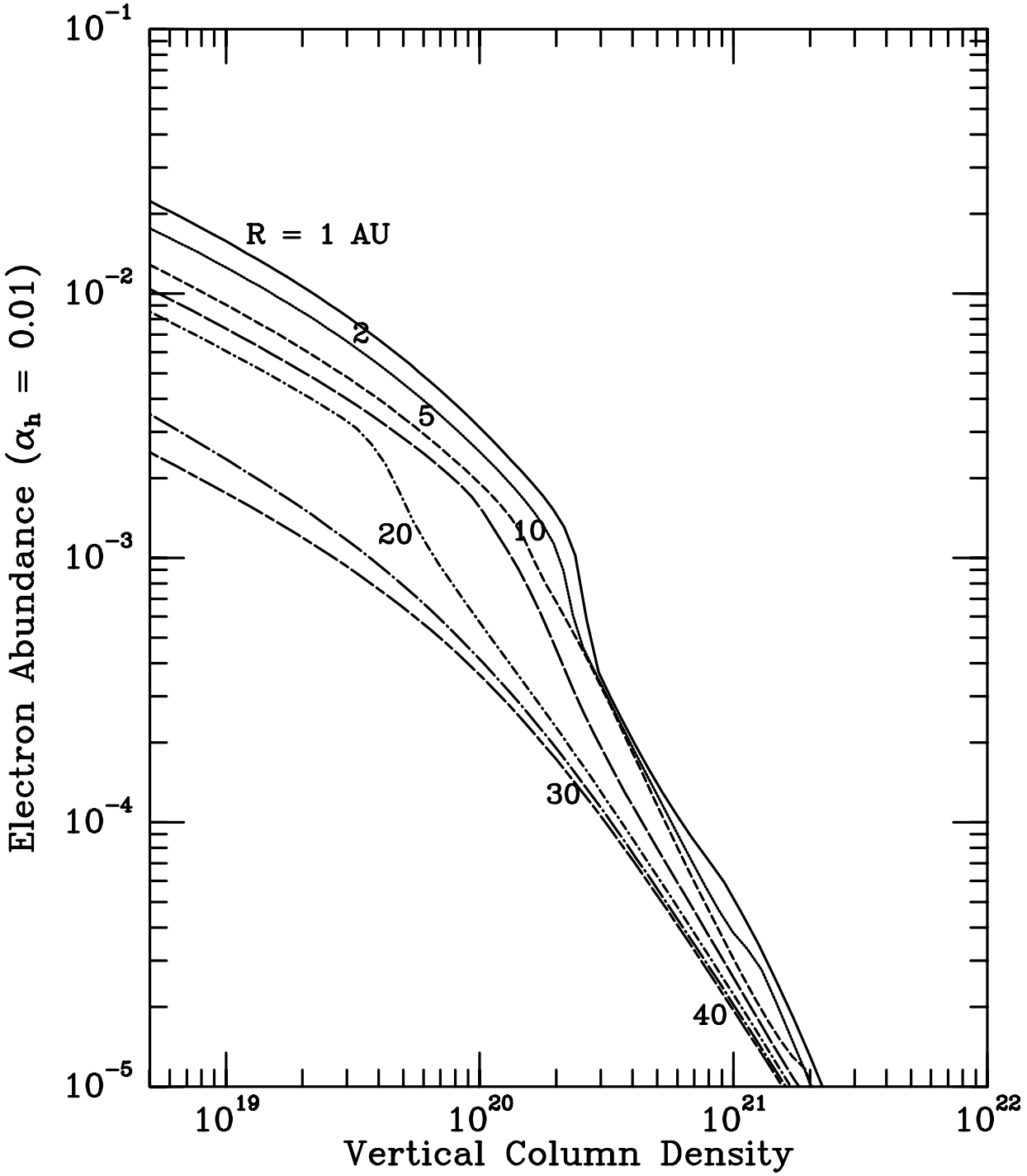
Electron Abundance (α_n = 0.01)
Vertical Column Density
R = 1 AU
2
5
10
20
30
40
10^{-1}
10^{-2}
10^{-3}
10^{-4}
10^{-5}
10^{19}
10^{20}
10^{21}
10^{22}

f3.eps

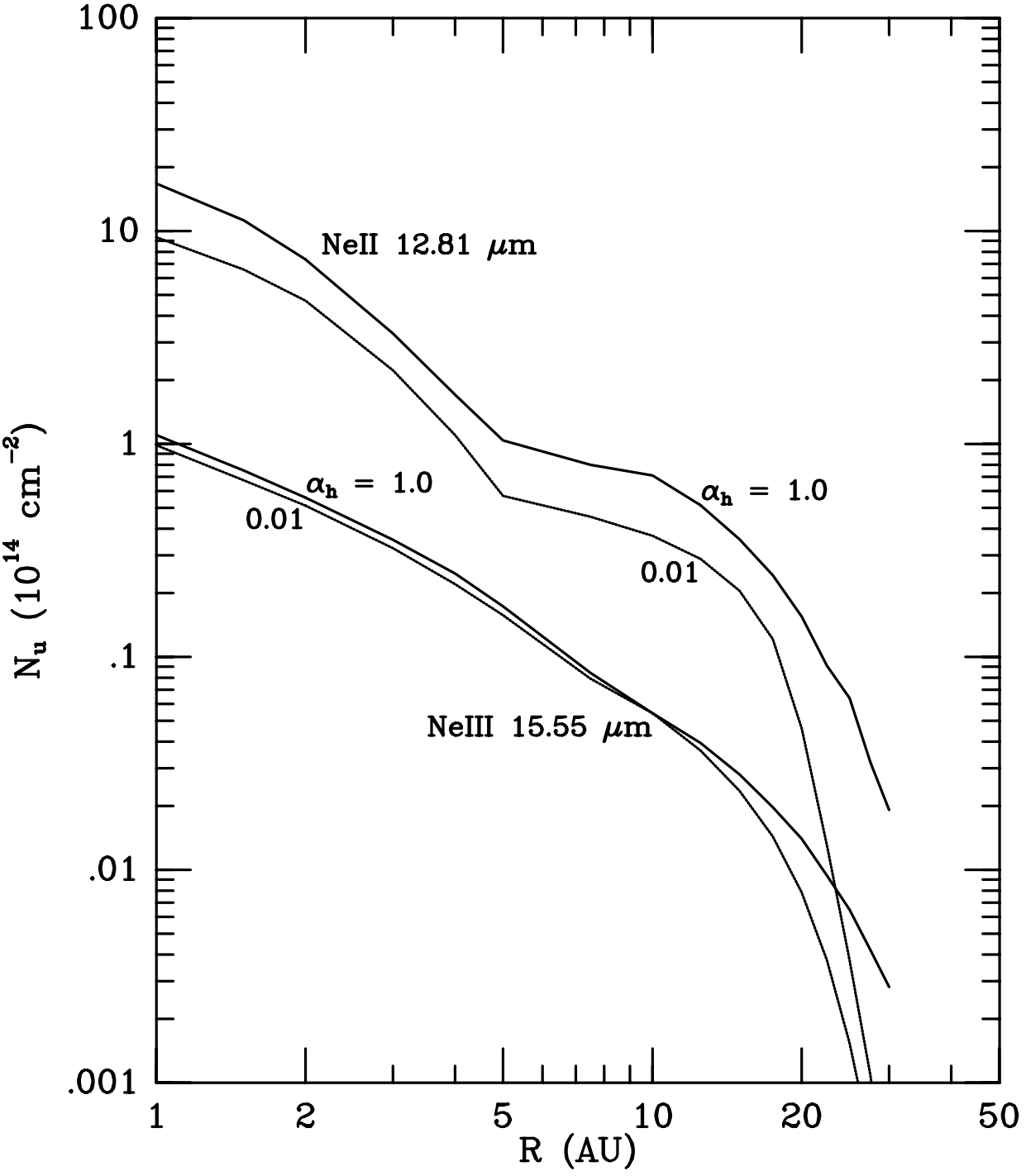
100
10
1
.1
.01
.001
1
2
5
10
20
50
R (AU)
N_u (10^{14} cm^{-2})
NeII 12.81 μm
NeIII 15.55 μm
α_h = 1.0
0.01
α_h = 1.0
0.01

f4.eps

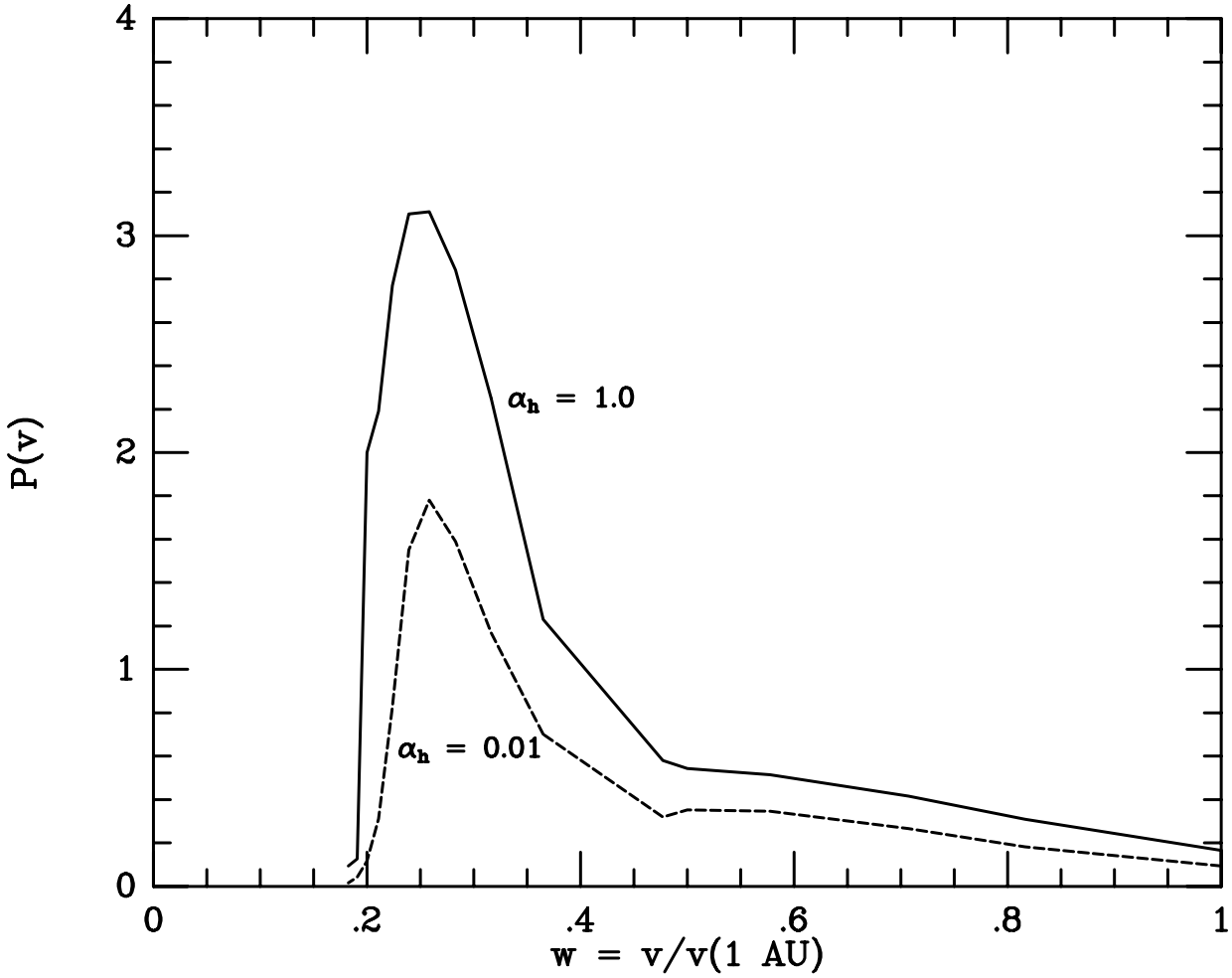

f5.eps